PRESSURE, TEMPERATURE AND IONIC STRENGTH EFFECTS ON THE WETTABILITY OF CO_2-BRINE-SANDSTONE SYSTEM: CORE-SCALE CONTACT ANGLE MEASUREMENTS

Ali Al-Menhali, Samuel Krevor

Department of Earth Science & Engineering, Qatar Carbonates and Carbon Storage Research Center, Imperial College London

This paper was prepared for presentation at the International Symposium of the Society of Core Analysts held in Napa Valley, California,, USA, 16-19 September, 2013

ABSTRACT

The wetting properties of CO_2-brine-rock systems will have a major impact on the management of CO_2 injection processes. The wettability of a system controls the flow and trapping efficiency during the storage of CO_2 in geological formations as well as the efficiency of enhanced oil recovery operations. While recent studies have shown CO_2 to generally act as a non-wetting phase in siliciclastic rocks, some observations report that the contact angle varies with pressure, temperature and water salinity. Additionally, there is a wide range of reported contact angles for this system, from strongly to weakly water-wet. In the case of some minerals, intermediate wet contact angles have been observed. Uncertainty with regard to the wetting properties of CO_2-brine systems is currently one of the remaining major unresolved issues with regards to reservoir management of CO_2 storage. In this study, we make semi-dynamic capillary pressure measurements of supercritical CO_2 and brine at reservoir conditions to observe shifts in the wetting properties. We utilize a novel core analysis technique recently developed by Pini et al [16] in 2012 to evaluate a core-scale effective contact angle by comparing Pc results with mercury intrusion capillary pressure measurements on the same rock. We evaluate wettability variation within a single rock with temperature, pressure, and salinity across a range of conditions relevant to subsurface CO_2 storage. This paper will include the initial results of measurements in a Berea sandstone sample across a wide range of conditions representative of subsurface reservoirs suitable for CO_2 storage (6-24 MPa, 25-120^{o}C, 0-5 mol kg^{-1}). The measurement uses X-ray CT imaging in a state of the art core flooding laboratory designed to operate at high temperature, pressure, and concentrated brines.

INTRODUCTION

Climate change is a major environmental challenge that we face today due to the increased anthropogenic emissions of greenhouse gases (GHG) to the atmosphere.

Carbon dioxide capture and storage (CCS) aims to safely sequester CO_2 generated from stationary sources, such as power-plants, into aquifers and depleted oil reservoirs. It is considered a valuable option to reduce of GHG and has been proposed as a practical technology to tackle climate change. Previously, carbon dioxide injection into the subsurface has mainly been used for enhanced oil recovery (EOR) purposes. Despite its utility in EOR and the continued development of CCS, little is currently known about the wetting properties of the CO_2-brine system on reservoir rocks, and no investigations have been performed assessing the impact of these properties on CO_2 flooding for CO_2 storage or EOR. The wetting properties of multiphase fluid systems in porous media have major impacts on the multiphase flow properties such as the capillary pressure and relative permeability. In this study, we develop an experimental setup that allows for making semi-dynamic capillary pressure measurement where CO_2 is injected at constant flow rate into a core that is initially fully saturated with water, while maintaining a constant outlet pressure. In this scenario, the pressure drop across the core corresponds to the capillary pressure at the inlet face of the core. When compared with mercury intrusion capillary pressure measurements, core-scale effective contact angle can be determined. In addition to providing a quantitative measure of the core-averaged wetting properties, the technique allows for the observation of shifts in contact angle with changing conditions. We examine the wettability changes of the CO_2-brine system in Berea sandstone with variations in reservoir conditions including supercritical, gaseous and liquid CO_2 injection. This paper includes the initial results of this study.

METHODOLOGY

Wettability can be measured by direct and indirect methods. Direct measurements include contact angle measurements made using the sessile drop techniques [4]. Indirect methods include the derivation of wettability indices based on the interpretation of observations of relative permeability, capillary pressure or spontaneous imbibition such as the Amott wettability index [2]. This study utilizes a novel technique that has been proposed recently by Pini et al. [16] to measure a core-averaged effective contact angle through the comparison of capillary pressure characteristic curves derived from two measurement techniques applied to the same sample. The first method is the widely applied mercury injection capillary pressure (MICP) measurement. The second is the semi-dynamic capillary pressure measurement. This technique is less commonly used but was developed by Lenormand et al. [10] in 1993 for oil and water and applied separately by Pini et al. [16] in 2012 for CO_2 and brine. The principles behind the semi-dynamic capillary pressure measurement are briefly reviewed here.

Semi-dynamic Capillary Pressure Measurement

The semi-dynamic capillary pressure measurement is best described by the steady-state injection of a non-wetting fluid through a core sample that is pre-saturated with a wetting fluid. The method is based on concepts developed for a steady state drainage relative

permeability measurement technique that exploits the presence of end-effects in a laboratory sample, [18]. A simplified schematic of the semi-dynamic core-flooding method is shown in Figure 1.

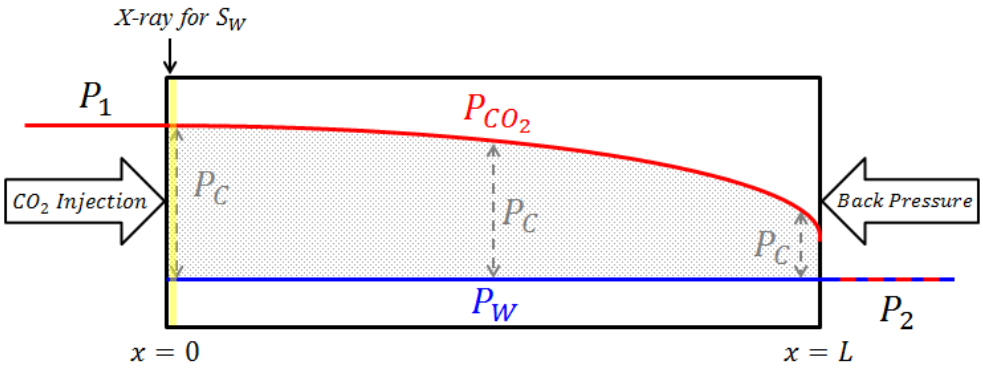

Figure 1. A schematic adapted from Pini et al. [16] of the semi-dynamic core-flooding capillary pressure measurement method. Capillary pressure is represented by the gray shaded area across the core which is the pressure difference between the non-wetting, CO_2, and wetting, water, phases at any given location in the core sample. In this study, the capillary pressure and saturations are measure at the inlet face of the core as described below.

The core is initially fully saturated with the wetting phase, brine. The non-wetting phase, CO_2, is injected at a constant flow rate while maintaining a constant outlet pressure set at the experimental condition. The pressures [kPa] at the inlet (P_1) and the outlet (P_2) of the core are monitored with two pressure transducers located at the inlet and outlet end-caps. The inlet end-cap is in contact with CO_2 during injection and therefore P_1 is the CO_2 pressure at the inlet face of the core. The non-wetting phase, CO_2, pressure is highest at the inlet and decreases towards the outlet. The brine, as the wetting phase, is assumed to be connected throughout the core. With a connected but immobile brine phase, the pressure in the phase is assumed to be constant across the core and equal to P_2. The same assumption is made for other capillary pressure measurements techniques such as the porous plate [7,13] and fritted glass [3] techniques where a continuous contact of the displaced fluid across one end of the sample is maintained. The capillary pressure, P_c [kPa], is the difference in pressure between the CO_2 and brine phase and goes to zero outside the core, where there are no capillaries. This is known as the capillary end effect which is discussed extensively in the literature and observed in other core-flooding experiments of oil-water and gas-water displacements when maintaining water contact at the outlet [19,5,15,8]. The boundary condition at the outlet of the core in this study was controlled by attaching a brine reservoir to the outlet end-cap ($x = L$) that provides continuity in the brine pressure. The capillary pressure can thus be measured at the inlet face of the core where the pressure change from the inlet to the outlet, pressure drop, of the core is equivalent to the capillary pressure at the inlet face of the core as shown in Eq. (1).

$$\boldsymbol{\Delta P = P_1 - P_2 = P_c \ (at \ x = 0)} \tag{1}$$

Where $P_1 = P_{CO_2}$ at the inlet at $x = 0$ and $P_2 = P_w = P_{CO_2}$ at the outlet of the core at x = L. X-ray CT scanning is used to measure the saturations in this study. Pressures are measured at the same time as saturation measurements at the inlet face of the core. The concurrent measurements allow for a direct link between capillary pressure and saturation and a capillary pressure curve can therefore be constructed by repeating these measurements at increasing CO_2 flow rates. A constant pressure drop across the core should be maintained during the x-ray scan (typically 1 second to 1 minute) to link the true saturation of each capillary pressure measurement. In this study, we assume that the fluid configurations in the pore space are controlled by the Young-Laplace equation, Eq. (2). We also assume that there is a direct correspondence between capillary pressure and saturation in the pore space [3]. This also implies that there is no difference between measurements carried out with two fluids in motion and measurements made with quasi-static capillary equilibrium conditions.

$$\boldsymbol{P_c = \frac{2\sigma cos\theta}{r}} \tag{2}$$

Here P_c [kPa] is the capillary pressure, σ [mN/m] is the interfacial tension, θ [degrees] is the contact angle measured in the wetting phase, and r [μm] is the pore-throat radius.

The flow rates were chosen carefully to allow for the measurement at a sufficient number of capillary pressures to generate a representative capillary pressure curve. To choose the flow rates, the MICP measurements of the sample were used along with an estimated relative permeability curve to estimate a priori the pressure drop (and thus P_c) for a given flow rate. The dimensionless capillary number, *Nc*, defined in Eq. (3), was used to ensure that local capillary equilibrium conditions applied during all of the experimental flow rates.

$$\boldsymbol{N_c = \frac{V\mu}{\sigma cos\theta}} \tag{3}$$

Where V [m/s] and μ [Pa s] are the CO_2 superficial velocity and dynamic viscosity, respectively, σ [N/m] is the interfacial tension between CO_2 and brine, and θ [degrees] is the contact angle. Capillary numbers around 10^{-4}-10^{-5} indicate that viscous and capillary forces are equivalent for the reservoir rock [6]. In this study, the capillary number for the highest flow rate was less than 10^{-5} and the pore-scale fluid distribution was thus controlled by capillary forces. Under this condition, Eq. (1) was applied for each flow rate to define the capillary pressure at the inlet of the core.

MICP and Core-scale Effective Contact Angle Measurements

Helium pycnometry was used on a plug sample taken from a slice adjacent to the inlet face of the core sample used in this study. This was to measure the true skeletal grain volume in order to correct for the pore volume not seen by mercury porosimetry measurements [17]. The same sub sample was then used for MICP measurements. MICP was used for two main purposes in this study. The first was to guide in the choice of appropriate flow rates during the core flood to create a representative capillary pressure

curve as described in the previous section. The second purpose was to measure the wetting properties of the core sample at different reservoir conditions. This was achieved by comparison of the capillary pressure curves obtained from mercury injection porosimetry and the semi-dynamic capillary pressure method. We can compare the measurements with the MICP data and treat the CO_2-brine contact angle in Eq. (4) as a fitting parameter. The contact angle value that provides the best fit for the semi-dynamic capillary pressure measurement represents the wetting property of the sample.

$$\boldsymbol{P_{C(CO_2/w)} = P_{C(Hg/a)} \frac{\sigma_{(CO_2/w)} \cos\theta_{(CO_2/w)}}{\sigma_{(Hg/a)} \cos\theta_{(Hg/a)}}} \quad (4)$$

Where the subscripts (CO_2/w) and (Hg/a) refer to the non-wetting and wetting phases of CO_2-brine and mercury-air, respectively. The mercury-air contact angle (measured in the wetting phase) and IFT applied were the customary values of 140° and 480 mN/m, respectively [20]. Carbon dioxide-brine interfacial tension (IFT) values for the experimental conditions were obtained from the correlation made by Li et al. [11] in 2012. The correlation covers the range of conditions investigated here.

MATERIALS

Rock Sample

The rock core sample used in this study was Berea sandstone. The core was relatively homogeneous with horizontal bedding planes along the core. The sample was fired at 700°C for 4 hours to stabilize clays. The length and diameter of the core are 8 and 1.5 inches, respectively. The faces of the core were machined flat to ensure good contact with the end-caps. The sample was vacuum dried for at least one day at 100°C before each experiment. The absolute permeability of the sample to water was 73 mD.

Fluids

CO_2 with 99.9% purity (BOC Industrial Gases, UK) and brine were used in this study. The aqueous solution had a total salt molality of 1 mol/kg of NaCl.

Table 1. Experimental conditions and fluids properties in this study

Molality [mol/kg]	Temperature [deg °C]	Pressure [MPa]	IFT[a] [mN/m]	CO_2/brine density[bc] [kg/m^3]	CO_2/brine viscosity[bc] [cP]
1	60	14	34.5	561 / 1017	0.042 / 0.524

[a] IFT values [11]

[b] Brine densities and viscosities [9]

[c] CO_2 densities and viscosities [12]

Core-flooding Experimental Setup

Capillary pressure measurements have been made in a state of the art core-flooding laboratory that has been developed at Imperial College. The experimental setup is designed to replicate in-situ conditions of up to 150°C and 30 MPa. A schematic of the flow loop system is shown in Figure 2. The setup includes six high precision pumps, an accurate temperature control system, an x-ray CT scanner that allows experiments to be performed in both vertical and horizontal directions, and real time data monitoring of pressures, volumes, flow rates, and temperatures across the system.

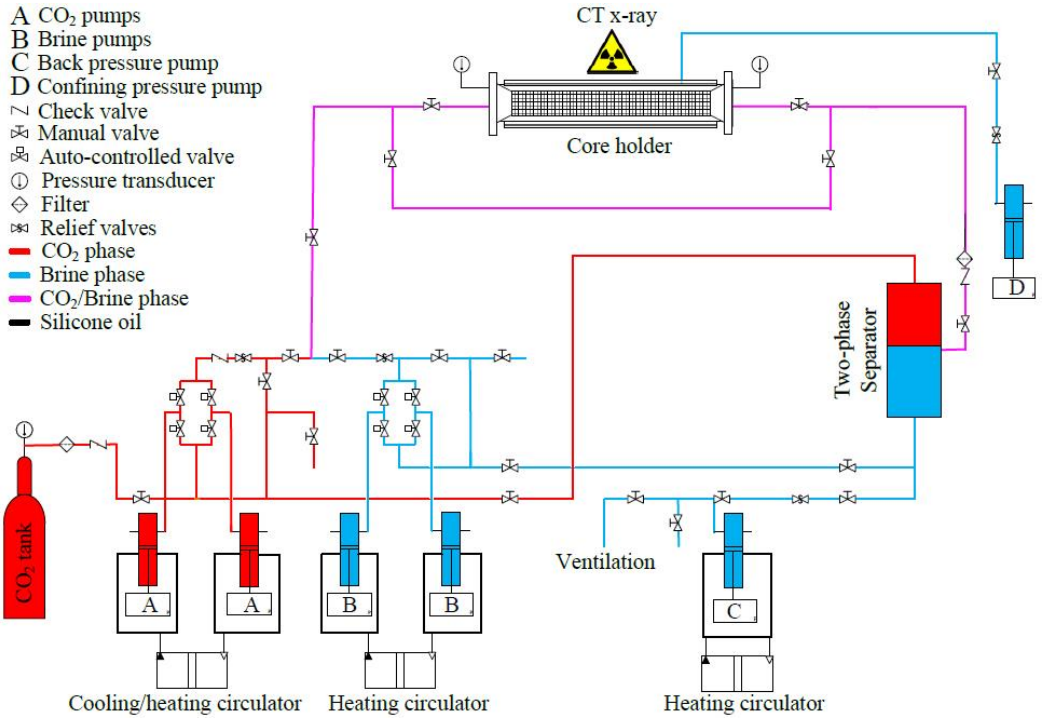

Figure 2. Schematic of core flooding apparatus used in this study

The main components of the experimental setup consisted of an aluminium core holder (Phoenix Instruments) that accommodates samples of 1.5 inch in diameter and lengths up to 10 inches, a back pressure pump, two gas pumps and two brine pumps (Teledyne Isco, Model 500HP) that allowed for continuous CO_2 and brine injection into the core sample at controlled constant flow rates, a confining pressure pump (Teledyne Isco, Model 100DX) to maintain a constant confining pressure around the sample, and a two-phase separator (HP/HT Separator, Vinci Technologies) that separated CO_2 and brine after exiting the core. All five pumps were heated to experimental temperature (Heating Circulation Thermostat, Huber). Electric heaters and high temperature insulation controlled the temperature in the tubing of the flow loop. The core sample was isolated from the confining fluid (brine) by a layering from the core outward (heat-shrinkable Teflon/nickel foil/ heat-shrinkable Teflon/ rubber sleeve). The core was then positioned between two Hastelloy steel end-caps. The end-caps had interconnected circular grooves for the purpose of distributing the injected fluid over the complete cross-sectional area of

the core sample face during injection. Each of the end-caps had two ports. In both the inlet and outlet a flow line was connected to one port and a high accuracy pressure transducer (Oil filled Digiquartz, Model 410K-HT-101, Paroscientific, Inc.) was connected to the other. Connecting the pressure transducers directly to the end-caps allowed for more precision in pressure readings and eliminated the noise otherwise generated when connected to a flow line. This was especially important when measuring low capillary pressure points where the pressure difference between the inlet and the outlet was very small. The core holder was positioned horizontally through the medical x-ray CT scanning instrument (HD-350E, Universal Systems) and used to measure the sample porosity and fluid saturations during the core-flooding experiment.

EXPERIMENTAL PROCEDURE

MICP Measurements

Helium pycnometry and mercury porosimetry were performed on the same sub-sample (~ 0.8 cm^3). Helium pycnometer measurements using an AccuPyc 1330 by Micromeritics were performed first to measure the true skeletal grain volume. The bulk volume of the sample was measured as the first stage in the MICP test. The mercury porosimetry instrument used in this test was an AutoPore IV by Micromeritics. The mercury-air capillary pressure was converted to CO_2-brine capillary pressure by using the appropriate IFT and θ values of each experimental condition. This was obtained on the basis of the same pore-throat radius relationship in the Young-Laplace Eq. (4).

Absolute Permeability Measurements

Absolute permeability to water was measured for each experimental condition. Permeability was measured by injecting water through the fully water-saturated core sample at a constant flow rate and recording the pressure drop across the core. Darcy's law was then used to calculate the permeability.

Fluid Circulation and CO_2 Saturated Brine Equilibration

The main steps for brine and CO_2 circulation are described in this section. The first step was to expel air from the flow loop by flowing CO_2 through all parts of the experimental setup at an elevated pressure and exhausting to the atmosphere. Then the system was pressurized with CO_2 and heated to the experimental pressure and temperature. This step was required to obtain the CO_2 saturated core background scan. Next, brine was injected into the loop to displace and dissolve all of the CO_2 out of the core at experimental pressure and temperature. A scan of the brine saturated core was obtained for porosity measurements. Then brine and CO_2 were circulated at experimental conditions in a closed loop bypassing the core. Carbon dioxide dissolved into the brine until equilibration was reached. This avoided any mass transfer between the phases during the

flooding and created a system of immiscible displacement. Mass balances of the fluid phases were maintained during the experiment and equilibration was confirmed after the stabilization of the volume of each fluid in the system was observed. At this point, the CO_2 flow was stopped and only CO_2 equilibrated brine was circulated. Then the CO_2 equilibrated brine was injected through the line into the core. Several pore volumes of brine were injected into the core sample to displace the initial brine with brine equilibrated with CO_2. This was confirmed by taking x-ray scans during injection until a slight increase in CT number corresponding to the higher density brine was observed distributed evenly along the core. Once the core is fully saturated with CO_2 equilibrated brine, another background x-ray CT scan is taken of the core.

Porosity and Fluid Saturations Using X-ray CT Scanning

Water porosity and experimental fluid saturations were measured for each experimental condition. Both porosity and saturation measurements were obtained by a combination of background and experimental X-ray scans [21,1]. The x-ray imaging parameters applied in this study were as follows: a voxel dimension of about (0.23x0.23x1) mm^3, a display field of view of 12 cm, an energy level of the radiation of 120 keV and a tube current of 225 mA. The porosity was measured by using four sets of x-ray scans. The first two were a scan of the air and a scan of the experimental brine at ambient conditions. The brine scans were made for every experiment so that the CT number of each particular brine-saturated core was obtained. The third scan was a scan of the dry core at ambient conditions where the pore space was filled with air. The fourth was a scan of the core saturated with brine at experimental conditions. The same confining pressure was applied in last two scans. The porosity was then calculated using Eq. (5).

$$\emptyset = \frac{CT_{brine} - CT_{dry}}{I_{brine} - I_{air}} \tag{5}$$

Where CT and I are the x-ray CT scanner attenuation coefficient converted to numerical values in Hounsfield units. These values were assigned for each voxel in the X-ray image. CT_{brine} and CT_{dry} were scan values from the brine saturated core and the dry core, respectively. I_{brine} and I_{air} were scan values obtained from scanning brine and air alone, respectively.

Fluid saturations measurements in the core sample required two background scans in addition to the experimental scan. The background scans were a scan of the core saturated with CO_2 and a scan of the core saturated with CO_2 equilibrated brine. Both scans were taken at experimental conditions and with confining pressure. Carbon dioxide saturation during CO_2 flow was calculated using Eq. (6).

$$S_{CO_2} = \frac{CT_{exp} - CT_{brine+CO_2}}{CT_{CO_2} - CT_{brine+CO_2}} \tag{6}$$

Where the subscripts exp, CO_2 and $brine + CO_2$ refer to scan values obtained during CO_2 injection through the core during core-flooding, while the core was saturated with

CO_2 and while the core was saturated with CO_2 equilibrated brine, respectively. The slice-averaged porosity and saturation properties were calculated using slice-averaged CT numbers. A total of 20 scans were taken for each set of CT numbers used in Eqs. (5) and (6). The repeated scans were then averaged to reduce the uncertainty associated to the computed porosities and saturations [16].

Core-flooding CO_2-Brine Capillary Pressure Measurements

The first semi-dynamic capillary pressure experiment was performed at the experimental condition described in Table 1. The core outlet was held at a pressure of 14 MPa. A confining pressure equal to 19 MPa was applied to the core resulting in a differential radial stress of 5 MPa. Carbon dioxide and brine were pre-equilibrated and the core sample was fully saturated with CO_2 equilibrated brine at experimental pressure and temperature. The core-flooding capillary pressure experiment was initiated by injecting 100% CO_2 into the core. Carbon dioxide injection flow rates ranged from 0.1 to 50 ml/min. This range allowed for observations covering a satisfactory portion of the capillary pressure curve with maximum values reaching more than 200 kPa. For each capillary pressure measurement, CO_2 was injected at a constant flow rate until a constant pressure drop across the core was reached. Then, an X-ray scan was performed at the inlet face of the core sample. It is essential to achieve constant pressure during the X-ray scan to link the correct saturation with the associated capillary pressure measurement. As described earlier, 20 scans were taken of the inlet slice and then averaged for each saturation measurement to reduce the uncertainty associated with the computed saturations.

RESULTS

Figure 3 and Figure 4 show the initial set of results of experiments designed to examine the wetting properties at different reservoir conditions. Figure 3 represent the slice-averaged CO_2 saturation profiles along the length of the core at each injection flow rate applied to generate capillary pressure points. The saturation profiles are smooth and an indication of the relatively homogenous Berea core sample used in this study. The negative saturation gradient towards the outlet is a result of the capillary end effect that propagates back into the core. Figure 4 shows the semi-dynamic CO_2-brine Pc observations measured at the inlet face of the core as well as MICP curves. A stable pressure drop was achieved for each CO_2 injection flow rate before taking x-ray scans to measure saturations. An effective core-scale contact angle of 50^o was applied in Eq. (4) to fit the MICP curve with the core flooding capillary pressure observations performed at the experimental condition described in Table 1. MICP curves of 40^o and 60^o were also plotted to show the sensitivity of Pc curves to contact angle. The horizontal and vertical error bars of the semi-dynamic Pc measurements represent pressure uncertainty caused by fluctuations during X-ray imaging time and saturation uncertainty based on the range of saturations seen from 20 repeated scans, respectively.

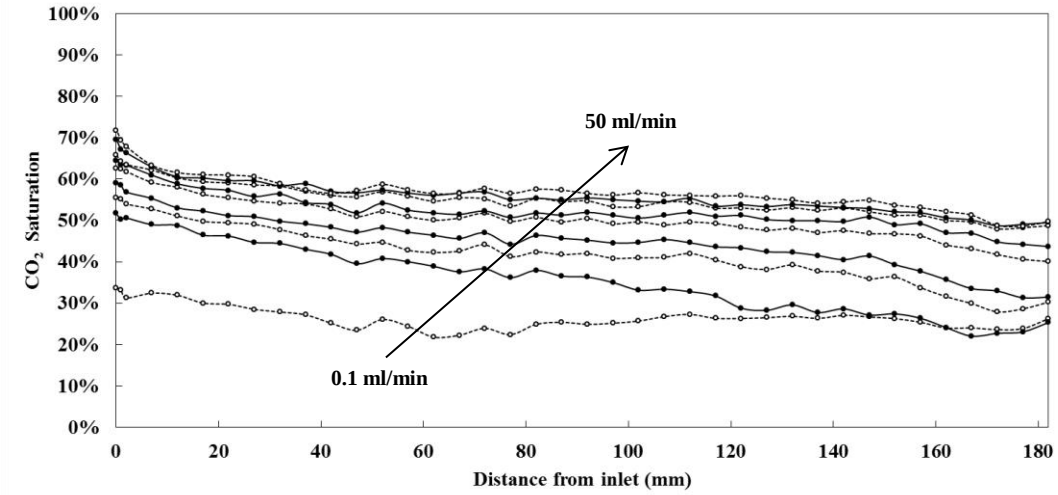

Figure 3. Slice-averaged CO_2 saturation profiles along the length of the core at different injection flow rates

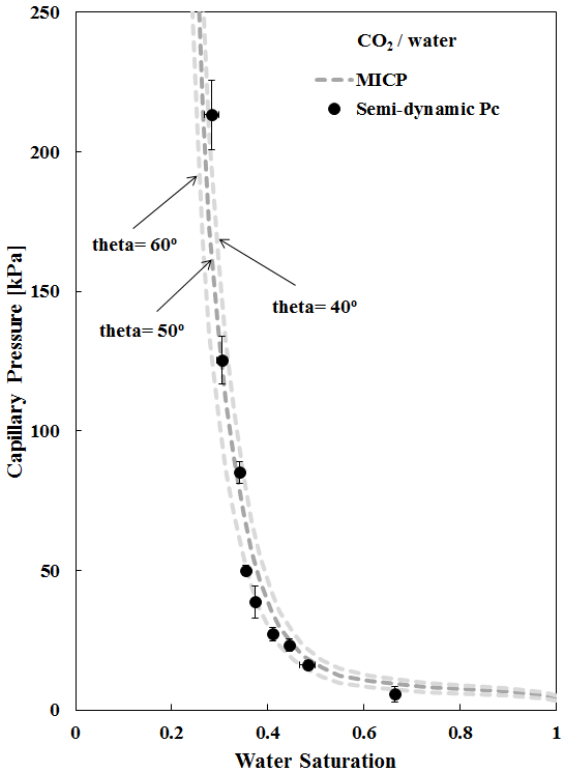

Figure 4. Black circles are results from the semi-dynamic CO_2-brine capillary pressure experiment, while the dotted lines represents MICP curves converted to the CO_2-brine system scaled by IFT of 34.5 mN/m and best fit contact angle of 50^o and +/- 10^o sensitivity range. The vertical and horizontal error bars represent pressure error within each scan and saturation error from 20 repeated scans, respectively.

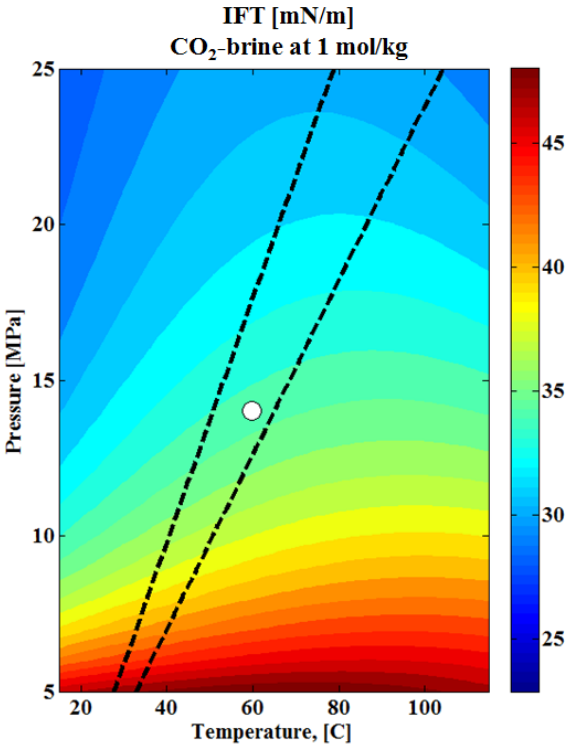

Figure 5. Contours show interfacial tension of CO_2-brine at 1 mol/kg [11]. The experimental condition is shown by the white circle. The dotted black lines represent the range of US geothermal and hydrostatic gradient [14] assuming a surface temperature of 15^oC and a hydrostatic pressure gradient.

CONCLUSION

Wettability determines the efficiency of enhanced oil recovery operations as well as our ability to inject and store CO_2 in geological formations. This study utilized a novel technique to produce an effective core-scale contact angle measurement. Further measurements will be made at a wide range of reservoir conditions to observe the impact of pressure, temperature and brine salinity on the wetting properties of the CO_2-brine system in siliciclastic rocks.

ACKNOWLEDGEMENT

We gratefully acknowledge funding from the Qatar Carbonates and Carbon Storage Research Centre (QCCSRC), provided jointly by Qatar Petroleum, Shell, and Qatar Science & Technology Park.

REFERENCES

1. Akin, S., A. Kovscek. "Computed Tomography in Petroleum Engineering Research." *Geological Society, London, Special Publications* 215, no. 1 (2003): 23-38.
2. Amott, E. "Observations Relating to the Wettability of Porous Rock." *Trans. AIME* 216 (1959): 156–62.
3. Brown, H. "Capillary Pressure Investigations." *Journal of Petroleum Technology* 3, no. 3 (1951): 67-74.
4. Chiquet, P., D. Broseta, and S. Thibeau. "Wettability Alteration of Caprock Minerals by Carbon Dioxide." *Geofluids* 7, no. 2 (2007): 112-22.
5. Hadley, G., L Handy. "A Theoretical and Experimental Study of the Steady State Capillary End Effect." Paper presented at the Fall Meeting of the *Petroleum Branch of AIME*, 1956.
6. Hassanizadeh, S., W. Gray. "Thermodynamic Basis of Capillary Pressure in Porous Media." *Water Resources Research* 29, no. 10 (1993): 3389-405.
7. Hassler, G., E. Brunner. "Measurement of Capillary Pressures in Small Core Samples." *Trans. AIME* 160, no. 3 (1945): 114-23.
8. Huang, D., M. Honarpour. "Capillary End Effects in Coreflood Calculations." *Journal of Petroleum Science and Engineering* 19, no. 1 (1998): 103-17.
9. Kestin, J., H. Khalifa, R. Correia. "Tables of the Dynamic and Kinematic Viscosity of Aqueous Nacl Solutions in the Temperature Range 20-150 C and the Pressure Range 0.1-35 Mpa." *American Chemical Society and the American Institute of Physics for the National Bureau of Standards*, 1981.
10. Lenormand, R., A. Eisenzimmer, C. Zarcone. "A Novel Method for the Determination of Water/Oil Capillary Pressures of Mixed-Wettability Samples." Paper presented at the *Soc. Core Analyst Conf.* Paper, 1993.
11. Li, X., E. Boek, G. Maitland, J. P. M. Trusler. "Interfacial Tension of (Brines + CO_2): (0.864 NaCl + 0.136 KCl) at Temperatures between (298 and 448) K, Pressures

between (2 and 50) Mpa, and Total Molalities of (1 to 5) Mol·Kg–1." *Journal of Chemical & Engineering Data* 57, no. 4 (2012): 1078-88.
12. Lemmon E., M. McLinden, D. Friend. "Thermophysical Properties of Fluid Systems" in "NIST Chemistry WebBook", NIST Standard Reference Database Number 69, Eds. P. Linstrom and W. Mallard, National Institute of Standards and Technology, Gaithersburg MD, 20899, http://webbook.nist.gov, (retrieved May 6, 2013).
13. McCullough, J., F. Albaugh, P. Jones. "Determination of the Interstitial-Water Content of Oil and Gas Sand by Laboratory Tests of Core Samples." *Drilling and Production Practice* (1944).
14. Nathenson, M., and M. Guffanti. "Geothermal Gradients in the Conterminous United States." *Journal of Geophysical Research: Solid Earth (1978–2012)* 93, no. B6 (1988): 6437-50.
15. Perkins Jr, F. "An Investigation of the Role of Capillary Forces in Laboratory Water Floods." *Journal of Petroleum Technology* 9, no. 11 (1957): 49-51.
16. Pini, R., S. Krevor, and S. Benson. "Capillary Pressure and Heterogeneity for the CO_2/Water System in Sandstone Rocks at Reservoir Conditions." *Advances in Water Resources* 38 (2012): 48-59.
17. Pini, R., S. Benson. "Simultaneous Determination of Capillary Pressure and Relative Permeability Curves from Core-Flooding Experiments with Various Fluid Pairs." *Water Resources Research* 49, doi:10.1002 (2013): wrcr.20274.
18. Ramakrishnan, T., A. Cappiello. "A New Technique to Measure Static and Dynamic Properties of a Partially Saturated Porous Medium." *Chemical Engineering Science* 46, no. 4 (1991): 1157-63.
19. Richardson, J., J. Kerver, J. Hafford, J. Osoba. "Laboratory Determination of Relative Permeability." *Journal of Petroleum Technology* 4, no. 8 (1952): 187-96.
20. Ritter, H., L. Drake. "Pressure Porosimeter and Determination of Complete Macropore-Size Distributions." *Industrial & Engineering Chemistry Analytical Edition* 17, no. 12 (1945): 782-86.
21. Withjack, E. "Computed Tomography for Rock-Property Determination and Fluid-Flow Visualization." *SPE formation evaluation* 3, no. 4 (1988): 696-704.